University of South Australia

School of Electrical and Information Engineering

Three-Phase Squirrel-Cage Induction Motor Drive Analysis Using LabVIEW™

NUR HAKIMAH AB AZIZ

A Thesis Submitted in Partial Fulfilment of the Requirement for the Award of the Degree of Master Engineering (Electrical Power Engineering)

July 2006

ABSTRACT

This thesis will present three-phase squirrel-cage induction motor drive simulators using the graphical-language (G-language) of LabVIEW™. Either *abc* or quadrature, direct and zero (*qd0*) machine models will be used in conjunction with sinusoidal and non-sinusoidal supplies. Non-sinusoidal supplies will include three types of voltage source inverters (VSIs), namely, 1) six-step inverter with 180° conduction angle, 2) six-step inverter with 120° conduction angle and 3) sinusoidal pulse-width-modulated (PWM) inverter. Two separate simulators are developed; one for the supply of the motor from a sinusoidal voltage source, the other from various types of non-sinusoidal voltage source. The mathematical models of the induction machine used in [1] have been adopted for the implementation. Those mathematical models are in the form of differential equations and are solved using Runge Kutta 4^{th} order method. The performance of induction machine drive is then presented into a set of output graphs. These output graphs permit the analysis of stator and rotor currents, stator and rotor flux linkages, electromagnetic torque, rotor speed and torque-speed characteristics. LabVIEW™ has been chosen as the platform of this project because it is a flexible programming language combined with built-in tools designed specifically for test, measurement and control.

CHAPTER 1

Introduction

1.1 Evolution of Electrical Drive Technology

The technology of electrical drive has begun almost two centuries ago [1]. The history of electrical motor started when Hans Christian Oersted discovered the magnetic effect of an electric current in 1820. In the following year, Michael Faraday discovered the electromagnetic rotation and built the first primitive direct current (DC) motor. Faraday went on to discover electromagnetic induction in 1831, but it was not until 1883 that Tesla invented the alternating current (AC) asynchronous motor [2].

Currently, the main types of electric motors are still the same, DC, AC asynchronous and synchronous, are all based on Oersted, Faraday and Tesla's theories. Historically, DC motor, with its mechanical commutator and brushes, was the undisputed choice in industrial application, primarily due to its inherent ability to provide independent torque and speed control. AC asynchronous motor, also named induction motor, though very rugged and easier to construct, their torque and speed control are more complicated. Induction motors are perhaps the most widely used of all electric motors. They offer reasonable asynchronous performance [3]: a manageable torque-speed curve, stable operation under load and generally satisfactory efficiency.

On an application where dynamic control is not an issue, the control requirement of the AC machine drive has been done using constant *volts/hertz* (V/f) technique. However, through the advancements of induction motor modelling, power electronic devices and microprocessors, the development of high performance AC drives has become a reality [4]. Since that, two types of high performance AC drive, field oriented and direct torque control drives have found a place in various applications that previously have been dominated and reserved for DC motors and drive systems.

1.2 DC Drives

DC drives are used extensively in variable-speed drives because of their variable characteristics. DC motors can provide a high starting torque and it is also possible to obtain speed control over a wide range. Also, the methods of speed control are normally simpler and less expensive than those of AC motors [5].

In DC motor, the magnetic field is created by the current through the field winding in the stator. This field is always at right angles to the field created by the armature winding. This condition, known as field orientation, is needed to generate maximum torque. The commutator-brush assembly in the DC motor has ensures that this condition will be maintained regardless of the rotor position. Once field orientation is achieved, the DC motor's torque can be controlled directly by only varying the armature current and by keeping the magnetising current constant. The torque response is fast since it can be changed instantaneously by controlling the current supplied by the source [6].

However, the main drawback of the DC motor is the uses of brushes and commutators have reduced the reliability of the DC motor. Since brushes and commutators will wear down, regular servicing is could not be avoided. Due to commutators, DC motors are not suitable for very high speed applications and require more maintenance than do AC motors [5-7].

1.3 AC Drives

The evolution of AC drive technology has been partly driven by the desire to emulate the performance of the DC drive, such as fast torque response and speed accuracy, while maintaining the advantages offered by the standard AC induction motor which is robust, simple in design, low cost, light and compact. Rashid [5] has outlined several advantages of AC drives which are lightweight, inexpensive and have low maintenance compared to DC drives.

For variable-speed applications, AC motors require power converters and AC voltage controllers in order to control frequency, voltage and current. These power controllers,

which are relatively complex and more expensive, require advanced feedback control techniques such as model reference, adaptive control, sliding mode control and field-oriented control. However, the advantages of AC drives outweigh the disadvantages. There are two types of AC drives namely, synchronous motor drives and induction motor drives [5, 8].

1.3.1 Synchronous motor drives

A brief explanation about synchronous motors is available in [5]. Synchronous motors have a polyphase winding on the stator, also known as armature, and a field winding carrying DC current on the rotor. There are two magnetomotive forces (MMF) involved; one due to the field current and the other due to the armature current. The resultant MMF produces the torque. The armature is identical to the stator of induction motors, but there is no induction in the rotor.

A synchronous motor is a constant-speed machine and always rotates with zero slip at the synchronous speed, which depends on the frequency and the number of poles. A synchronous motor can be operated as a motor or generator. The power factor (PF) can be controlled by varying the field current. With cycloconverters and inverters, the applications of synchronous motors in variable-speed drives are widening.

1.3.2 Induction motor drives

The three-phase induction motor is the work-horse of modern industry. Three-phase induction motors are commonly used in adjustable-speed drives and they have three-phase stator and rotor windings. There are two common types of induction machines, namely, squirrel-cage and wound-rotor.

Squirrel-cage induction motors have a cylindrical rotor with short-circuited rotor windings with the voltage supplied to stator windings. The rotor does not have a brush and commutator but consists of conducting bars that are placed into the rotor slots. These bars are shorted by the shorting rings [1].

In contrast, the wound-rotor induction motors have wye-connected rotor windings. In addition to the voltage that is applied to the stator windings, the phase voltages can be supplied to the rotor windings using brushes and slip rings. Thus, torque-speed characteristic could be shaped [1].

However, wound-rotor induction motors have not been widely used because their efficiency and maximal angular velocity are lower compared to squirrel-cage. On the other hand, squirrel-cage induction motors have been tremendously used in high-performance electric drives and electromechanical systems. Therefore, in the case of the simulator developed by the author and presented in this thesis, only three-phase squirrel-cage induction motor drive will be presented.

1.4 Power Electronic Devices

Power electronic circuits are principally concerned with processing energy. They convert electrical energy from the form supplied by a source to the form required by a load. These conversions are permitted by the switching characteristics of the power devices. The power electronics circuits can be classified into four types [9, 10]:

(i) AC-DC converters

An AC-DC converter in which energy flows from the AC network to the DC network is called a rectifier.

(ii) DC-DC converters

The DC-DC converter takes the DC output of the AC-DC converter and transforms it to the different DC voltages required by the electronics. In relatively high power applications, such as traction, the DC-DC converter is known as a *chopper*.

(iii) AC-AC converters

This converter is used to obtain a variable AC output voltage from a fixed AC source. This type of converter is also known as AC voltage controller.

(iv) DC-AC converters

DC-AC converters are also known as inverter. The function of an inverter is to change a DC input voltage to a symmetrical AC output voltage of desired magnitude and frequency. The output voltage could be fixed or variable at a fixed or variable frequency. Inverters can be broadly classified either as voltage source inverters (VSIs) or current-source inverters (CSIs).

1.5 LabVIEW™

LabVIEW™ has been used as the platform in this project. LabVIEW™ is a modern graphical programming language that is especially useful for controlling equipments and instruments such as those used in research laboratories. Furthermore, LabVIEW™ is a scientific and engineering rapid application development environment specialized towards data acquisition, electronic measurement and control applications [11]. LabVIEW™ can be used to handle data acquisition in easier way compared to text based programming language. It is known that fully functional data acquisition program can be created in just 90 seconds [12].

LabVIEW™ programs are called virtual instruments (VIs) [13]. Basically, there are three main parts of a VI which are the front panel, the block diagram and the icon. The main purposes of the front panel are to get the input values and to view the outputs from the VI block diagram. Each front panel has an accompanying block diagram. The block diagram can be assumed as source code. Finally, the function of the icon is to turn a VI into an object that can be used in the block diagrams of other VIs as if it were a subroutine.

1.6 Objective of the Thesis

The objective of the thesis is to build user friendly simulators in order to analyse the transient behaviour and steady-state performance of a three-phase squirrel-cage induction motor drive. The simulators are also to serve as a teaching and learning aid in electrical machine courses.

1.7 Structure of the Thesis

The work presented in this thesis is organised in five main chapters. These five chapters are structured as follows:

Chapter 1 reviews the evolution of electrical drive technology. A brief description about LabVIEW™ is also discussed.

Chapter 2 describes the dynamic modeling of three-phase squirrel-cage induction motors using *abc* and quadrature, direct and zero (*qd0*) quantities as well as non-sinusoidal supplies from voltage source inverters (VSIs).

Chapter 3 covers a general description of the design of the VI in order to associate the modelling of induction motor with graphic programming of the VI.

Chapter 4 discusses performance analysis of electrical drives with different configurations using the simulators designed.

Finally, Chapter 5 gives the conclusions of the thesis and the suggestion for further work as an extension of this study.

All the block diagrams of the simulators are shown in Appendices.

CHAPTER 2

Three-Phase Squirrel-Cage Induction Motor Drive

2.1 Introduction

This chapter presents an overview of the principle of three-phase squirrel-cage induction motor drive. First, the model and the related equations of three-phase induction machine are described and presented in both *abc* and quadrature, direct and zero (*qd0*) machine models. Then the operation principles of six-step and pulsed-width-modulated (PWM) inverters are discussed.

2.2 Dynamic Model of Induction Machine

The steady state model of induction motor, which is represented by a steady equivalent circuit shown in Figure 2.1 [5], describes only a steady state behavior of the induction motor. It was used when steady state analyses, such as efficiency, losses, steady state torque, currents and fluxes are need to be evaluated. Designing the machine drives based on this model will only produced a drive that normally has a poor transient performance [14]. When machine drives for high performance application need to be designed, a model that can describe the transient as well as the steady state behavior of the induction machine is needed. Therefore, by using the dynamic model, the transient behavior of the induction motor, which can not be analysed using steady state equivalent model, can be predicted and studied.

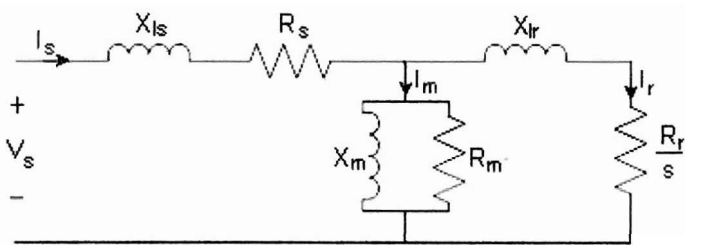

Figure 2.1: Per-phase steady state equivalent circuit of induction motor [5]

In developing the dynamic model of the induction motor, a few assumptions are made [2, 15]. These assumptions will only simplify the analysis and at the same time will not affect the validity of the develop model.

(i) The induction machine is considered as symmetrical two poles, three phase windings.

(ii) The winding on the stator is symmetrically distributed such that the spatial magnetomotive force (MMF) produced is sinusoidal.

(iii) The surface windings have negligible depth. The core is assumed to have infinite permeability. Hysteresis, eddy current and slotting effects can be neglected.

The cross section of the machine with the above assumption is shown in Figure 2.2 [1]. The magnetic axes of the stator is represented by *as*, *bs* and *cs* while magnetic axes of the rotor is represented by *ar*, *br* and *cr*. The angle between the rotor and stator axis is indicated by θ_r. The mathematical model of three-phase induction machines using machine variables has been derived in detail in [1].

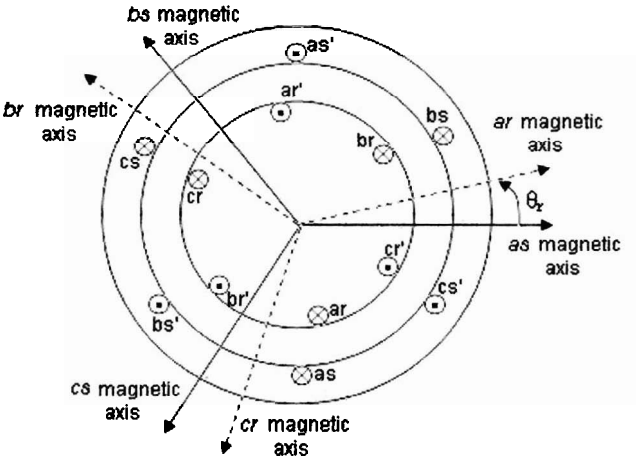

Figure 2.2: Cross-section of elementary symmetrical three-phase induction motor [1]

2.2.1 *abc* machine model[1]

This section develops the mathematical model of three-phase induction motors using machine variables. The goal is to find a set of differential equations to map the dynamics of induction machines in order to perform a thorough analysis of the transient behavior and steady-state performance.

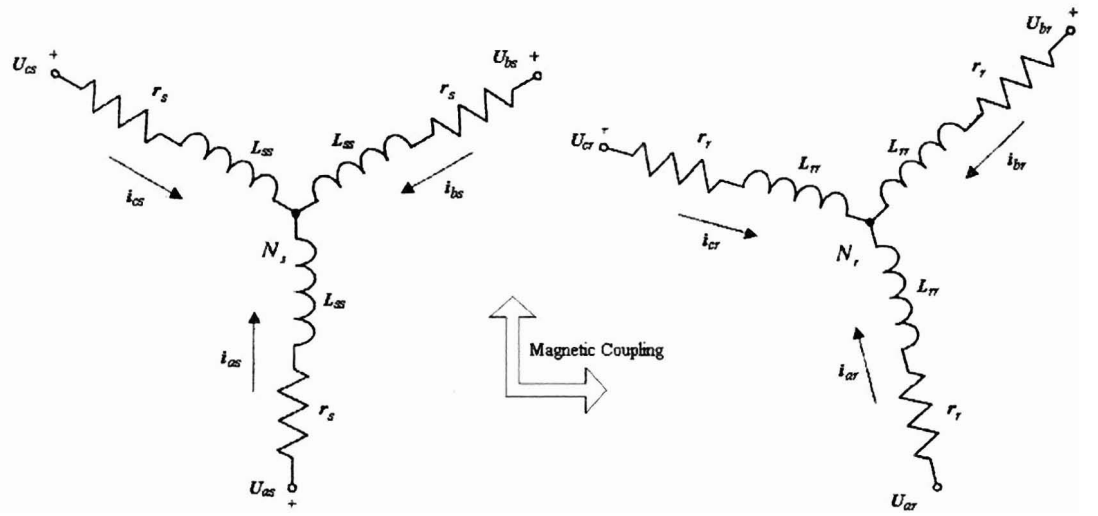

Figure 2.3: Three-phase symmetrical induction motor [1]

[1] The mathematical models presented here are adopted from [1]. All rotor parameters are referred to the stator.

From Figure 2.3 [1], Kirchoff's voltage law is applied to give a set of two matrix differential equations for the voltages that is applied to the *abc* stator and rotor windings, the *abc* stator and rotor currents, and flux linkages. With rotor parameters are referred to the stator,

$$\begin{aligned} \mathbf{u}_{abcs} &= \mathbf{r}_s \mathbf{i}_{abcs} + \frac{d\boldsymbol{\psi}_{abcs}}{dt} \\ \mathbf{u}_{abcr} &= \mathbf{r}_r \mathbf{i}_{abcr} + \frac{d\boldsymbol{\psi}_{abcr}}{dt} \end{aligned} \tag{1}$$

where the *abc* stator and rotor voltages, currents and flux linkages are given in vector form,

$$\mathbf{u}_{abcs} = \begin{bmatrix} u_{as} \\ u_{bs} \\ u_{cs} \end{bmatrix}, \mathbf{u}_{abcr} = \begin{bmatrix} u_{ar} \\ u_{br} \\ u_{cr} \end{bmatrix}, \mathbf{i}_{abcs} = \begin{bmatrix} i_{as} \\ i_{bs} \\ i_{cs} \end{bmatrix}, \mathbf{i}_{abcr} = \begin{bmatrix} i_{ar} \\ i_{br} \\ i_{cr} \end{bmatrix}, \boldsymbol{\psi}_{abcs} = \begin{bmatrix} \psi_{as} \\ \psi_{bs} \\ \psi_{cs} \end{bmatrix} \text{ and } \boldsymbol{\psi}_{abcr} = \begin{bmatrix} \psi_{ar} \\ \psi_{br} \\ \psi_{cr} \end{bmatrix}$$

In Eq. (1), the diagonal matrices of the stator and rotor resistances are expressed as

$$\mathbf{r}_s = \begin{bmatrix} r_s & 0 & 0 \\ 0 & r_s & 0 \\ 0 & 0 & r_s \end{bmatrix} \text{ and } \mathbf{r}_r = \begin{bmatrix} r_r & 0 & 0 \\ 0 & r_r & 0 \\ 0 & 0 & r_r \end{bmatrix}$$

The flux linkages are found using the corresponding currents in the stator and rotor windings and self and mutual inductances. The stator and rotor self inductances are

$$\begin{aligned} L_{ss} &= L_{ls} + L_{ms} \\ L_{rr} &= L_{lr} + L_{ms} \end{aligned} \tag{2}$$

where L_{ls} and L_{lr} are stator and rotor leakage inductances while L_{ms} is stator magnetising inductance. The matrices of self and mutual inductances between the stator windings, $\mathbf{L}_s$, and rotor windings, $\mathbf{L}_r$, are found to be

$$\mathbf{L}_s = \begin{bmatrix} L_{ls} + L_{ms} & -\frac{1}{2}L_{ms} & -\frac{1}{2}L_{ms} \\ -\frac{1}{2}L_{ms} & L_{ls} + L_{ms} & -\frac{1}{2}L_{ms} \\ -\frac{1}{2}L_{ms} & -\frac{1}{2}L_{ms} & L_{ls} + L_{ms} \end{bmatrix} \tag{3}$$

and

$$\mathbf{L}_r = \begin{bmatrix} L_{lr} + L_{ms} & -\frac{1}{2}L_{ms} & -\frac{1}{2}L_{ms} \\ -\frac{1}{2}L_{ms} & L_{lr} + L_{ms} & -\frac{1}{2}L_{ms} \\ -\frac{1}{2}L_{ms} & -\frac{1}{2}L_{ms} & L_{lr} + L_{ms} \end{bmatrix} \tag{4}$$

An assumption is made that the mutual inductances between the stator and rotor windings are sinusoidal functions of the rotor angular displacement, θ_r. Hence,

$$\mathbf{L}_{sr} = L_{ms} \begin{bmatrix} \cos\theta_r & \cos\left(\theta_r + \frac{2}{3}\pi\right) & \cos\left(\theta_r - \frac{2}{3}\pi\right) \\ \cos\left(\theta_r - \frac{2}{3}\pi\right) & \cos\theta_r & \cos\left(\theta_r + \frac{2}{3}\pi\right) \\ \cos\left(\theta_r + \frac{2}{3}\pi\right) & \cos\left(\theta_r - \frac{2}{3}\pi\right) & \cos\theta_r \end{bmatrix} \tag{5}$$

In particular, the analysis of the stator and rotor magnetically coupled system, which can be accomplished using Figure 2.3, leads to the following set of equations

$$\begin{aligned} \boldsymbol{\psi}_{abcs} &= \mathbf{L}_s \mathbf{i}_{abcs} + \mathbf{L}_{sr} \mathbf{i}_{abcr} \\ \boldsymbol{\psi}_{abcr} &= \mathbf{L}^T{}_{sr} \mathbf{i}_{abcs} + \mathbf{L}_r \mathbf{i}_{abcr} \end{aligned} \tag{6}$$

From Eq. (6), explicit expressions for derivatives of Eq. (1) can be found.

$$\mathbf{u}_{abcs} = \mathbf{r}_s \mathbf{i}_{abcs} + \frac{d\boldsymbol{\psi}_{abcs}}{dt} = \mathbf{r}_s \mathbf{i}_{abcs} + \mathbf{L}_s \frac{d\mathbf{i}_{abcs}}{dt} + \frac{d(\mathbf{L}_{sr}\mathbf{i}_{abcr})}{dt}$$

$$\mathbf{u}_{abcr} = \mathbf{r}_r \mathbf{i}_{abcr} + \frac{d\boldsymbol{\psi}_{abcr}}{dt} = \mathbf{r}_r \mathbf{i}_{abcr} + \mathbf{L}_r \frac{d\mathbf{i}_{abcr}}{dt} + \frac{d(\mathbf{L}_{sr}^T \mathbf{i}_{abcs})}{dt} \tag{7}$$

Hence, the following sets of voltage equations are obtained.

$$\begin{aligned}
u_{as} &= r_s i_{as} + (L_{ls} + L_{ms})\frac{di_{as}}{dt} - \frac{1}{2}L_{ms}\frac{di_{bs}}{dt} - \frac{1}{2}L_{ms}\frac{di_{cs}}{dt} + L_{ms}\cos\theta_r \frac{di_{ar}}{dt} + L_{ms}\cos\left(\theta_r + \frac{2\pi}{3}\right)\frac{di_{br}}{dt} \\
&\quad + L_{ms}\cos\left(\theta_r - \frac{2\pi}{3}\right)\frac{di_{cr}}{dt} - L_{ms}\left[i_{ar}\sin\theta_r + i_{br}\sin\left(\theta_r + \frac{2\pi}{3}\right) + i_{cr}\sin\left(\theta_r - \frac{2\pi}{3}\right)\right]\omega_r \\
u_{bs} &= r_s i_{bs} - \frac{1}{2}L_{ms}\frac{di_{as}}{dt} + (L_{ls} + L_{ms})\frac{di_{bs}}{dt} - \frac{1}{2}L_{ms}\frac{di_{cs}}{dt} + L_{ms}\cos\left(\theta_r - \frac{2\pi}{3}\right)\frac{di_{ar}}{dt} + L_{ms}\cos\theta_r \frac{di_{br}}{dt} \\
&\quad + L_{ms}\cos\left(\theta_r + \frac{2\pi}{3}\right)\frac{di_{cr}}{dt} - L_{ms}\left[i_{ar}\sin\left(\theta_r - \frac{2\pi}{3}\right) + i_{br}\sin\theta_r + i_{cr}\sin\left(\theta_r + \frac{2\pi}{3}\right)\right]\omega_r \\
u_{cs} &= r_s i_{cs} - \frac{1}{2}L_{ms}\frac{di_{as}}{dt} - \frac{1}{2}L_{ms}\frac{di_{bs}}{dt} + (L_{ls} + L_{ms})\frac{di_{cs}}{dt} + L_{ms}\cos\left(\theta_r + \frac{2\pi}{3}\right)\frac{di_{ar}}{dt} + L_{ms}\cos\left(\theta_r - \frac{2\pi}{3}\right)\frac{di_{br}}{dt} \\
&\quad + L_{ms}\cos\theta_r \frac{di_{cr}}{dt} - L_{ms}\left[i_{ar}\sin\left(\theta_r + \frac{2\pi}{3}\right) + i_{br}\sin\left(\theta_r - \frac{2\pi}{3}\right) + i_{cr}\sin\theta_r\right]\omega_r \\
u_{ar} &= r_r i_{ar} + L_{ms}\cos\theta_r \frac{di_{as}}{dt} + L_{ms}\cos\left(\theta_r - \frac{2\pi}{3}\right)\frac{di_{bs}}{dt} + L_{ms}\cos\left(\theta_r + \frac{2\pi}{3}\right)\frac{di_{cs}}{dt} + (L_{lr} + L_{ms})\frac{di_{ar}}{dt} \\
&\quad - \frac{1}{2}L_{ms}\frac{di_{br}}{dt} - \frac{1}{2}L_{ms}\frac{di_{cr}}{dt} - L_{ms}\left[i_{as}\sin\theta_r + i_{bs}\sin\left(\theta_r - \frac{2\pi}{3}\right) + i_{cs}\sin\left(\theta_r + \frac{2\pi}{3}\right)\right]\omega_r \\
u_{br} &= r_r i_{br} + L_{ms}\cos\left(\theta_r + \frac{2\pi}{3}\right)\frac{di_{as}}{dt} + L_{ms}\cos\theta_r \frac{di_{bs}}{dt} + L_{ms}\cos\left(\theta_r - \frac{2\pi}{3}\right)\frac{di_{cs}}{dt} - \frac{1}{2}L_{ms}\frac{di_{ar}}{dt} \\
&\quad + (L_{lr} + L_{ms})\frac{di_{br}}{dt} - \frac{1}{2}L_{ms}\frac{di_{cr}}{dt} - L_{ms}\left[i_{as}\sin\left(\theta_r + \frac{2\pi}{3}\right) + i_{bs}\sin\theta_r + i_{cs}\sin\left(\theta_r - \frac{2\pi}{3}\right)\right]\omega_r \\
u_{cr} &= r_r i_{cr} + L_{ms}\cos\left(\theta_r - \frac{2\pi}{3}\right)\frac{di_{as}}{dt} + L_{ms}\cos\left(\theta_r + \frac{2\pi}{3}\right)\frac{di_{bs}}{dt} + L_{ms}\cos\theta_r \frac{di_{cs}}{dt} - \frac{1}{2}L_{ms}\frac{di_{ar}}{dt} \\
&\quad - \frac{1}{2}L_{ms}\frac{di_{br}}{dt} + (L_{lr} + L_{ms})\frac{di_{cr}}{dt} - L_{ms}\left[i_{as}\sin\left(\theta_r - \frac{2\pi}{3}\right) + i_{bs}\sin\left(\theta_r + \frac{2\pi}{3}\right) + i_{cs}\sin\theta_r\right]\omega_r
\end{aligned} \tag{8}$$

Eq. (8) is rearranged into Cauchy's form and is implemented for performance analysis of induction machines.

$$
\begin{bmatrix} \frac{di_{as}}{dt} \\ \frac{di_{bs}}{dt} \\ \frac{di_{cs}}{dt} \\ \frac{di_{ar}}{dt} \\ \frac{di_{br}}{dt} \\ \frac{di_{cr}}{dt} \end{bmatrix} = \frac{1}{L_{\Sigma L}} \begin{bmatrix} -r_s L_{\Sigma m} & -\frac{1}{2} r_s L_{ms} & -\frac{1}{2} r_s L_{ms} & 0 & 0 & 0 \\ -\frac{1}{2} r_s L_{ms} & -r_s L_{\Sigma m} & -\frac{1}{2} r_s L_{ms} & 0 & 0 & 0 \\ -\frac{1}{2} r_s L_{ms} & -\frac{1}{2} r_s L_{ms} & -r_s L_{\Sigma m} & 0 & 0 & 0 \\ 0 & 0 & 0 & -r_r L_{\Sigma m} & -\frac{1}{2} r_r L_{ms} & -\frac{1}{2} r_r L_{ms} \\ 0 & 0 & 0 & -\frac{1}{2} r_r L_{ms} & -r_r L_{\Sigma m} & -\frac{1}{2} r_r L_{ms} \\ 0 & 0 & 0 & -\frac{1}{2} r_r L_{ms} & -\frac{1}{2} r_r L_{ms} & -r_r L_{\Sigma m} \end{bmatrix} \begin{bmatrix} i_{as} \\ i_{bs} \\ i_{cs} \\ i_{ar} \\ i_{br} \\ i_{cr} \end{bmatrix}
$$

$$
+ \frac{1}{L_{\Sigma L}} \begin{bmatrix} 0 & 0 & 0 & r_r L_{ms} \cos A & r_r L_{ms} \cos B & r_r L_{ms} \cos C \\ 0 & 0 & 0 & r_r L_{ms} \cos C & r_r L_{ms} \cos A & r_r L_{ms} \cos B \\ 0 & 0 & 0 & r_r L_{ms} \cos B & r_r L_{ms} \cos C & r_r L_{ms} \cos A \\ r_s L_{ms} \cos A & r_s L_{ms} \cos C & r_s L_{ms} \cos B & 0 & 0 & 0 \\ r_s L_{ms} \cos B & r_s L_{ms} \cos A & r_s L_{ms} \cos C & 0 & 0 & 0 \\ r_s L_{ms} \cos C & r_s L_{ms} \cos B & r_s L_{ms} \cos A & 0 & 0 & 0 \end{bmatrix} \begin{bmatrix} i_{as} \\ i_{bs} \\ i_{cs} \\ i_{ar} \\ i_{br} \\ i_{cr} \end{bmatrix}
$$

$$
+ \frac{1}{L_{\Sigma L}} \begin{bmatrix} 0 & 1.3L_{ms}^2 \omega_r & -1.3L_{ms}^2 \omega_r & L_{\Sigma ms} \omega_r \sin A & L_{\Sigma ms} \omega_r \sin B & L_{\Sigma ms} \omega_r \sin C \\ -1.3L_{ms}^2 \omega_r & 0 & 1.3L_{ms}^2 \omega_r & L_{\Sigma ms} \omega_r \sin C & L_{\Sigma ms} \omega_r \sin A & L_{\Sigma ms} \omega_r \sin B \\ 1.3L_{ms}^2 \omega_r & -1.3L_{ms}^2 \omega_r & 0 & L_{\Sigma ms} \omega_r \sin B & L_{\Sigma ms} \omega_r \sin C & L_{\Sigma ms} \omega_r \sin A \\ L_{\Sigma ms} \omega_r \sin A & L_{\Sigma ms} \omega_r \sin C & L_{\Sigma ms} \omega_r \sin B & 0 & -1.3L_{ms}^2 \omega_r & 1.3L_{ms}^2 \omega_r \\ L_{\Sigma ms} \omega_r \sin B & L_{\Sigma ms} \omega_r \sin A & L_{\Sigma ms} \omega_r \sin C & 1.3L_{ms}^2 \omega_r & 0 & -1.3L_{ms}^2 \omega_r \\ L_{\Sigma ms} \omega_r \sin C & L_{\Sigma ms} \omega_r \sin B & L_{\Sigma ms} \omega_r \sin A & -1.3L_{ms}^2 \omega_r & 1.3L_{ms}^2 \omega_r & 0 \end{bmatrix} \begin{bmatrix} i_{as} \\ i_{bs} \\ i_{cs} \\ i_{ar} \\ i_{br} \\ i_{cr} \end{bmatrix}
$$

$$
+ \frac{1}{L_{\Sigma L}} \begin{bmatrix} 2L_{ms} + L_{lr} & \frac{1}{2} L_{ms} & \frac{1}{2} L_{ms} & -L_{ms} \cos A & -L_{ms} \cos B & -L_{ms} \cos C \\ \frac{1}{2} L_{ms} & 2L_{ms} + L_{lr} & \frac{1}{2} L_{ms} & -L_{ms} \cos C & -L_{ms} \cos A & -L_{ms} \cos B \\ \frac{1}{2} L_{ms} & \frac{1}{2} L_{ms} & 2L_{ms} + L_{lr} & -L_{ms} \cos B & -L_{ms} \cos C & -L_{ms} \cos A \\ -L_{ms} \cos A & -L_{ms} \cos C & -L_{ms} \cos B & 2L_{ms} + L_{lr} & \frac{1}{2} L_{ms} & \frac{1}{2} L_{ms} \\ -L_{ms} \cos B & -L_{ms} \cos A & -L_{ms} \cos C & \frac{1}{2} L_{ms} & 2L_{ms} + L_{lr} & \frac{1}{2} L_{ms} \\ -L_{ms} \cos C & -L_{ms} \cos B & -L_{ms} \cos A & \frac{1}{2} L_{ms} & \frac{1}{2} L_{ms} & 2L_{ms} + L_{lr} \end{bmatrix} \begin{bmatrix} u_{as} \\ u_{bs} \\ u_{cs} \\ u_{ar} \\ u_{br} \\ u_{cr} \end{bmatrix}
$$

(9)

where,

$$L_{\Sigma L} = \left(3L_{ms} + L_{lr}\right)L_{lr}, \quad L_{\Sigma m} = 2L_{ms} + L_{lr}, \quad L_{\Sigma ms} = \frac{3}{2}L_{ms}^2 + L_{ms}L_{lr},$$

$$A = \theta_r, \quad B = \left(\theta_r + \frac{2}{3}\pi\right), \text{ and } \quad C = \left(\theta_r - \frac{2}{3}\pi\right)$$

The expression for the torque developed by induction motor is obtained in order to find the net torque. The electromagnetic torque for a two poles three-phase induction machine is found using the expression for coenergy, W_c. In particular,

$$T_e = \frac{\partial W_c(\mathbf{i}_{abcs}, \mathbf{i}_{abcr}, \theta_r)}{\partial \theta_r} \tag{10}$$

where

$$W_c = \frac{1}{2}\mathbf{i}_{abcs}^T(\mathbf{L}_s - L_{ls}\mathbf{I})\mathbf{i}_{abcs} + \mathbf{i}_{abcs}^T\mathbf{L}_{sr}(\theta_r)\mathbf{i}_{abcr} + \frac{1}{2}\mathbf{i}_{abcr}^T(\mathbf{L}_r - L_{lr}\mathbf{I})\mathbf{i}_{abcr} \tag{11}$$

Solving Eq. (10) gives

$$T_e = -L_{ms}\left\{\begin{array}{l}\left[i_{as}\left(i_{ar} - \frac{1}{2}i_{br} - \frac{1}{2}i_{cr}\right) + i_{bs}\left(i_{br} - \frac{1}{2}i_{ar} - \frac{1}{2}i_{cr}\right) + i_{cs}\left(i_{cr} - \frac{1}{2}i_{br} - \frac{1}{2}i_{ar}\right)\right]\sin\theta_r \\ + \frac{\sqrt{3}}{2}\left[i_{as}\left(i_{br} - i_{cr}\right) + i_{bs}\left(i_{cr} - i_{ar}\right) + i_{cs}\left(i_{ar} - i_{br}\right)\right]\cos\theta_r\end{array}\right\} \tag{12}$$

The equations of motion consist the mechanical parameters namely, moment of inertia, J, friction and damping coefficient, B_m, and load torque, T_L, that describe the circuitry transient behaviour are given as

$$\frac{d\omega_r}{dt} = \frac{1}{J}\left(T_e - B_m\omega_r - T_L\right) \tag{13}$$

and

$$\frac{d\theta_r}{dt} = \omega_r \tag{14}$$

where ω_r is the rotor angular velocity. Substituting Eq. (12) into Eq. (13) gives

$$\frac{d\omega_r}{dt} = -\frac{1}{J}L_{ms}\left\{\left[i_{as}\left(i_{ar}-\frac{1}{2}i_{br}-\frac{1}{2}i_{cr}\right)+i_{bs}\left(i_{br}-\frac{1}{2}i_{ar}-\frac{1}{2}i_{cr}\right)+i_{cs}\left(i_{cr}-\frac{1}{2}i_{br}-\frac{1}{2}i_{ar}\right)\right]\sin\theta_r + \frac{\sqrt{3}}{2}\left[i_{as}\left(i_{br}-i_{cr}\right)+i_{bs}\left(i_{cr}-i_{ar}\right)+i_{cs}\left(i_{ar}-i_{br}\right)\right]\cos\theta_r\right\} - \frac{B_m}{J}\omega_r - \frac{T_L}{J} \quad (15)$$

2.2.2 *qd0* machine model[2]

Lyshevski [1] has stated that the quadrature, direct and zero (*qd0*) machine model can be applied to reduce the complexity of the resulting differential equations that map the dynamics of two-phase induction machines. In order to develop the mathematical model of three-phase induction motors in the stationary reference frame, three-phase induction machine with quadrature and direct magnetic axes is considered as shown in Figure 2.4 [1, 14]. The real and the imaginary axes of the stator are represented by *ds* and *qs*, while *dr* and *qr* are the real and the imaginary axis of the rotor.

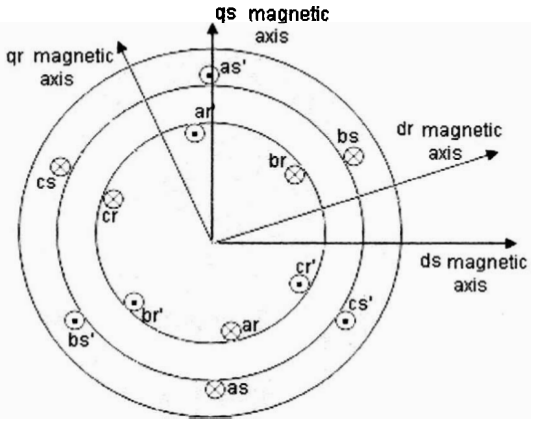

Figure 2.4: Cross-section of the two poles, three-phase winding induction motor [1,14]

[2] The mathematical models presented here are adopted from [1]. All rotor parameters referred to the stator in the stationary reference frame.

In the most general case, the model is developed in the arbitrary reference frame, and the frame angular velocity, ω, is not specified. Since stationary reference frame model is applied in this thesis, thus, the angular velocity is later to be assigned to zero, $\omega = 0$.

To transform the machine *abc* stator and rotor voltages, currents and flux linkages to the *qd0* axis components, the following transformations are used.

$$\begin{aligned}
\mathbf{u}_{qd0s} &= \mathbf{K}_s \mathbf{u}_{abcs} \\
\mathbf{i}_{qd0s} &= \mathbf{K}_s \mathbf{i}_{abcs} \qquad (16) \\
\boldsymbol{\psi}_{qd0s} &= \mathbf{K}_s \boldsymbol{\psi}_{abcs}
\end{aligned}$$

$$\begin{aligned}
\mathbf{u}_{qd0r} &= \mathbf{K}_r \mathbf{u}_{abcr} \\
\mathbf{i}_{qd0r} &= \mathbf{K}_r \mathbf{i}_{abcr} \qquad (17) \\
\boldsymbol{\psi}_{qd0r} &= \mathbf{K}_r \boldsymbol{\psi}_{abcr}
\end{aligned}$$

where the Park transformation matrix for stator and rotor, $\mathbf{K}_s$ and $\mathbf{K}_r$ are given as

$$\mathbf{K}_s = \frac{2}{3}\begin{bmatrix} \cos\theta & \cos\left(\theta - \frac{2}{3}\pi\right) & \cos\left(\theta + \frac{2}{3}\pi\right) \\ \sin\theta & \sin\left(\theta - \frac{2}{3}\pi\right) & \sin\left(\theta + \frac{2}{3}\pi\right) \\ \frac{1}{2} & \frac{1}{2} & \frac{1}{2} \end{bmatrix}$$

and

$$\mathbf{K}_r = \frac{2}{3}\begin{bmatrix} \cos(\theta - \theta_r) & \cos\left(\theta - \theta_r - \frac{2}{3}\pi\right) & \cos\left(\theta - \theta_r + \frac{2}{3}\pi\right) \\ \sin(\theta - \theta_r) & \sin\left(\theta - \theta_r - \frac{2}{3}\pi\right) & \sin\left(\theta - \theta_r + \frac{2}{3}\pi\right) \\ \frac{1}{2} & \frac{1}{2} & \frac{1}{2} \end{bmatrix}$$

In the stationary reference frame, one assigns $\omega = 0$, and thus, $\theta = 0$. Therefore, the matrix that needs to be applied in the stationary reference frame is found as

$$\mathbf{K}_s = \frac{2}{3}\begin{bmatrix} \cos\theta & \cos\left(\theta-\frac{2}{3}\pi\right) & \cos\left(\theta+\frac{2}{3}\pi\right) \\ \sin\theta & \sin\left(\theta-\frac{2}{3}\pi\right) & \sin\left(\theta+\frac{2}{3}\pi\right) \\ \frac{1}{2} & \frac{1}{2} & \frac{1}{2} \end{bmatrix}_{\theta=0} = \begin{bmatrix} \frac{2}{3} & -\frac{1}{3} & -\frac{1}{3} \\ 0 & -\frac{1}{\sqrt{3}} & \frac{1}{\sqrt{3}} \\ \frac{1}{3} & \frac{1}{3} & \frac{1}{3} \end{bmatrix} \tag{18}$$

From Eq. (16), stator voltages in *qd0* model are found to be

$$\begin{bmatrix} u_{qs} \\ u_{ds} \\ u_{0s} \end{bmatrix} = \begin{bmatrix} \frac{2}{3} & -\frac{1}{3} & -\frac{1}{3} \\ 0 & -\frac{1}{\sqrt{3}} & \frac{1}{\sqrt{3}} \\ \frac{1}{3} & \frac{1}{3} & \frac{1}{3} \end{bmatrix} \begin{bmatrix} u_{as} \\ u_{bs} \\ u_{cs} \end{bmatrix} \tag{19}$$

and can be simplified as

$$\begin{aligned} u_{qs}(t) &= \frac{2}{3}u_{as}(t) - \frac{1}{3}u_{bs}(t) - \frac{1}{3}u_{cs}(t) \\ u_{ds}(t) &= -\frac{1}{\sqrt{3}}u_{bs}(t) + \frac{1}{\sqrt{3}}u_{cs}(t) \\ u_{0s}(t) &= \frac{1}{3}u_{as}(t) + \frac{1}{3}u_{bs}(t) + \frac{1}{3}u_{cs}(t) \end{aligned} \tag{20}$$

The differential equations for the voltages from Eq. (1) can be transformed to *qd0* quantities by taking note the inverse Park transformation matrices, $\mathbf{K}_s^{-1}$ and $\mathbf{K}_r^{-1}$

$$\begin{aligned} \mathbf{K}_s^{-1}\mathbf{u}_{qd0s} &= \mathbf{r}_s\mathbf{K}_s^{-1}\mathbf{i}_{qd0s} + \frac{d\left(\mathbf{K}_s^{-1}\boldsymbol{\psi}_{qd0s}\right)}{dt} \\ \mathbf{K}_r^{-1}\mathbf{u}_{qd0r} &= \mathbf{r}_r\mathbf{K}_r^{-1}\mathbf{i}_{qd0r} + \frac{d\left(\mathbf{K}_r^{-1}\boldsymbol{\psi}_{qd0r}\right)}{dt} \end{aligned} \tag{21}$$

Multiplying left and right sides of Eq. (21) by $\mathbf{K}_s$ and $\mathbf{K}_r$, will finally results the voltage equations for stator and rotor circuits in the arbitrary reference frame,

$$\mathbf{u}_{qd0s} = \mathbf{r}_s \mathbf{i}_{qd0s} + \begin{bmatrix} 0 & \omega & 0 \\ -\omega & 0 & 0 \\ 0 & 0 & 0 \end{bmatrix} \boldsymbol{\psi}_{qd0s} + \frac{d\boldsymbol{\psi}_{qd0s}}{dt}$$

$$\mathbf{u}_{qd0r} = \mathbf{r}_r \mathbf{i}_{qd0r} + \begin{bmatrix} 0 & \omega - \omega_r & 0 \\ -\omega + \omega_r & 0 & 0 \\ 0 & 0 & 0 \end{bmatrix} \boldsymbol{\psi}_{qd0r} + \frac{d\boldsymbol{\psi}_{qd0r}}{dt} \tag{22}$$

The expressions for the *qd0* axis components of stator and rotor flux linkages must be derived in order to solve Eq. (22). Thus, Eq. (6) is represented using the *qd0* quantities of flux linkages by employing the Park transformation matrices.

$$\mathbf{K}_s^{-1} \boldsymbol{\psi}_{qd0s} = \mathbf{L}_s \mathbf{K}_s^{-1} \mathbf{i}_{qd0s} + \mathbf{L}_{sr} \mathbf{K}_r^{-1} \mathbf{i}_{qd0r}$$

$$\mathbf{K}_r^{-1} \boldsymbol{\psi}_{qd0r} = \mathbf{L}_{sr}^{T} \mathbf{K}_s^{-1} \mathbf{i}_{qd0s} + \mathbf{L}_r \mathbf{K}_r^{-1} \mathbf{i}_{qd0r} \tag{23}$$

Multiplying left and right sides of Eq. (23) by $\mathbf{K}_s$ and $\mathbf{K}_r$, will finally results the following flux linkage equations

$$\psi_{qs} = L_{ls} i_{qs} + M i_{qs} + M i_{qr}$$

$$\psi_{ds} = L_{ls} i_{ds} + M i_{ds} + M i_{dr} \tag{24}$$

$$\psi_{0s} = L_{ls} i_{0s}$$

$$\psi_{qr} = L_{lr} i_{qr} + M i_{qr} + M i_{qs}$$

$$\psi_{dr} = L_{lr} i_{dr} + M i_{dr} + M i_{ds} \tag{25}$$

$$\psi_{0r} = L_{lr} i_{0r}$$

where $M = \frac{3}{2} L_{ms}$.

Substituting Eqs. (24) and (25) into Eq. (22) will result the following differential equations in order to map three-phase induction motor circuitry dynamics in the arbitrary reference frame.

$$
\begin{aligned}
u_{qs} &= r_s i_{qs} + \omega\left(L_{ls} i_{ds} + M i_{ds} + M i_{dr}\right) + \frac{d\left(L_{ls} i_{qs} + M i_{qs} + M i_{qr}\right)}{dt} \\
u_{ds} &= r_s i_{ds} - \omega\left(L_{ls} i_{qs} + M i_{qs} + M i_{qr}\right) + \frac{d\left(L_{ls} i_{ds} + M i_{ds} + M i_{dr}\right)}{dt} \\
u_{0s} &= r_s i_{0s} + \frac{d\left(L_{ls} i_{0s}\right)}{dt} \\
u_{qr} &= r_r i_{qr} + \left(\omega - \omega_r\right)\left(L_{lr} i_{dr} + M i_{ds} + M i_{dr}\right) + \frac{d\left(L_{lr} i_{qr} + M i_{qs} M i_{qr}\right)}{dt} \\
u_{dr} &= r_r i_{dr} - \left(\omega - \omega_r\right)\left(L_{lr} i_{qr} + M i_{qs} + M i_{qr}\right) + \frac{d\left(L_{lr} i_{dr} + M i_{ds} M i_{dr}\right)}{dt} \\
u_{0r} &= r_r i_{0r} + \frac{d\left(L_{lr} i_{0r}\right)}{dt}
\end{aligned}
\tag{26}
$$

Since the stationary reference frame model of squirrel-cage induction motor is applied in this thesis, thus, the angular velocity and rotor voltages are equal to zero, $\omega = u_{qr} = u_{dr} = u_{or} = 0$. The Cauchy's forms of these differential equations are found to be

$$
\begin{aligned}
\frac{di_{qs}}{dt} &= \frac{1}{L_{SM} L_{RM} - M^2}\left[-L_{RM} r_s i_{qs} + M r_r i_{qr} - M\left(M i_{ds} + L_{RM} i_{dr}\right)\omega_r + L_{RM} u_{qs}\right] \\
\frac{di_{ds}}{dt} &= \frac{1}{L_{SM} L_{RM} - M^2}\left[-L_{RM} r_s i_{ds} + M r_r i_{dr} + M\left(M i_{qs} + L_{RM} i_{qr}\right)\omega_r + L_{RM} u_{ds}\right] \\
\frac{di_{0s}}{dt} &= \frac{1}{L_{ls}}\left[-r_s i_{0s} + u_{0s}\right] \\
\frac{di_{qr}}{dt} &= \frac{1}{L_{SM} L_{RM} - M^2}\left[M r_s i_{qs} - L_{SM} r_r i_{qr} + L_{SM}\left(M i_{ds} + L_{RM} i_{dr}\right)\omega_r - M u_{qs}\right] \\
\frac{di_{dr}}{dt} &= \frac{1}{L_{SM} L_{RM} - M^2}\left[M r_s i_{ds} - L_{SM} r_r i_{dr} - L_{SM}\left(M i_{qs} + L_{RM} i_{qr}\right)\omega_r - M u_{ds}\right] \\
\frac{di_{0r}}{dt} &= \frac{1}{L_{lr}}\left[-r_r i_{0r} + u_{0r}\right]
\end{aligned}
\tag{27}
$$

where $L_{SM} = L_{ls} + M = L_{ls} + \frac{3}{2}L_{ms}$ and $L_{RM} = L_{lr} + M = L_{lr} + \frac{3}{2}L_{ms}$

Again, the equations of motion are used to describe the circuitry transient behavior as mentioned earlier in section 2.2.1. First, the equation for the electromagnetic torque developed by three-phase induction motors is obtained using the *qd0*-axis components of stator and rotor currents. From Eqs. (10) and (11),

$$T_e = \left(\mathbf{K}_s^{-1}\mathbf{i}_{qd0s}\right)^T \frac{\partial \mathbf{L}_{sr}(\theta_r)}{\partial \theta_r}\mathbf{K}_r^{-1}\mathbf{i}_{qd0r} = \mathbf{i}_{qd0s}^T \mathbf{K}_s^{-1^T} \frac{\partial \mathbf{L}_{sr}(\theta_r)}{\partial \theta_r}\mathbf{K}_r^{-1}\mathbf{i}_{qd0r} \tag{28}$$

By performing multiplication of matrices, the following formula for the electromagnetic torque results

$$T_e = 1.5M\left(i_{qs}i_{dr} - i_{ds}i_{qr}\right) \tag{29}$$

Therefore, the equation of motion is now given as

$$\frac{d\omega_r}{dt} = \frac{1.5M}{J}\left(i_{qs}i_{dr} - i_{ds}i_{qr}\right) - \frac{B_m}{J}\omega_r - \frac{T_L}{J} \tag{30}$$

2.3 Power Converters of Induction Machine

The simulators developed by the author and presented in this thesis permit the analysis of induction machine drive from two types of supply, sinusoidal and non-sinusoidal. For sinusoidal supply, the following set of balanced three-phase voltage is applied to the *as*, *bs* and *cs* windings (refer Figure 2.2) in order to guarantee a balanced operating conditions.

$$\begin{aligned} u_{as}(t) &= V_m \cos(\omega_f t) \\ u_{bs}(t) &= V_m \cos\left(\omega_f t - \frac{2}{3}\pi\right) \\ u_{cs}(t) &= V_m \cos\left(\omega_f t + \frac{2}{3}\pi\right) \end{aligned} \tag{31}$$

where V_m is the peak voltage amplitude.

However, induction machine used in electric drives and servo-systems must be controlled. The angular velocity of squirrel-cage induction motors is regulated using power converters by changing the magnitude and frequency of the phase voltages applied to the stator windings. Figure 2.5 [1, 5, 7] shows the basic components of variable-frequency converters which are rectifier, filter and inverter.

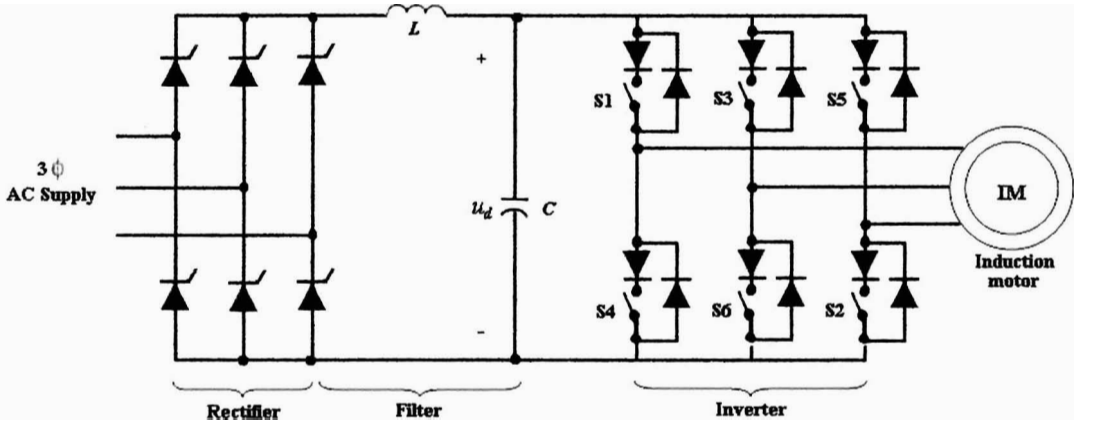

Figure 2.5: Variable frequency power converters and induction motor [1, 5, 7]

Polyphase rectifiers are always used to control medium and high power induction motors. Polyphase rectifiers contain several ac sources and the rectified voltage is summated at the output. The rectified voltage is filtered to reduce the harmonic content of the rectifier output voltage. Passive and active harmonic reduction, harmonic elimination and harmonic cancellation can be attained using passive and active filters. In addition, a stiff DC bus voltage, u_d, is maintained by the use of a large capacitor in DC link [1].

Inverters are used to control the output frequency and to convert the DC voltage to a variable frequency AC voltage. The inverter of Figure 2.5 used thyristor as switching device instead of transistors. Bose [1, 7] pointed out that thyristors have one important advantage over transistors, which is their ability to withstand a substantial fault current for a brief time before protective devices (fuses or circuit breakers) operate. However, thyristors require external commutation circuitry because they are not inherently capable of turn-off. The external device is not shown in Figure 2.5.

For non-sinusoidal supplies, six-step and PWM inverters are applied in this thesis. A three-phase output can be obtained from a configuration of six thyristors and six diodes as shown in Figure 2.5. For six-step inverter, two types of control signals can be applied to the thyristor, 180° or 120° conduction angle respectively. Rashid [5] has emphasised that the 180° conduction has better utilisation of the switches and is the preferred method. However, in the case of simulator presented in this thesis, both methods are applicable.

2.3.1 Six-step inverter with 180° conduction angle

Referring to Figure 2.5, each thyristor conducts at 180° and is numbered in the sequence of switching. Three thyristors remain on at any instant of time. There are six modes of operation in a cycle and the duration of each mode is 60°. In order to obtain three-phase balanced voltages, the sequence of switching is in the order of 5-6-1, 6-1-2, 1-2-3, 2-3-4, 3-4-5, 4-5-6 and back to 5-6-1 as shown in Figure 2.6(a). This results in the line-to-line voltage waveforms as shown in Figure 2.6(b) where u_d is the DC voltage from the filter of Figure 2.5.

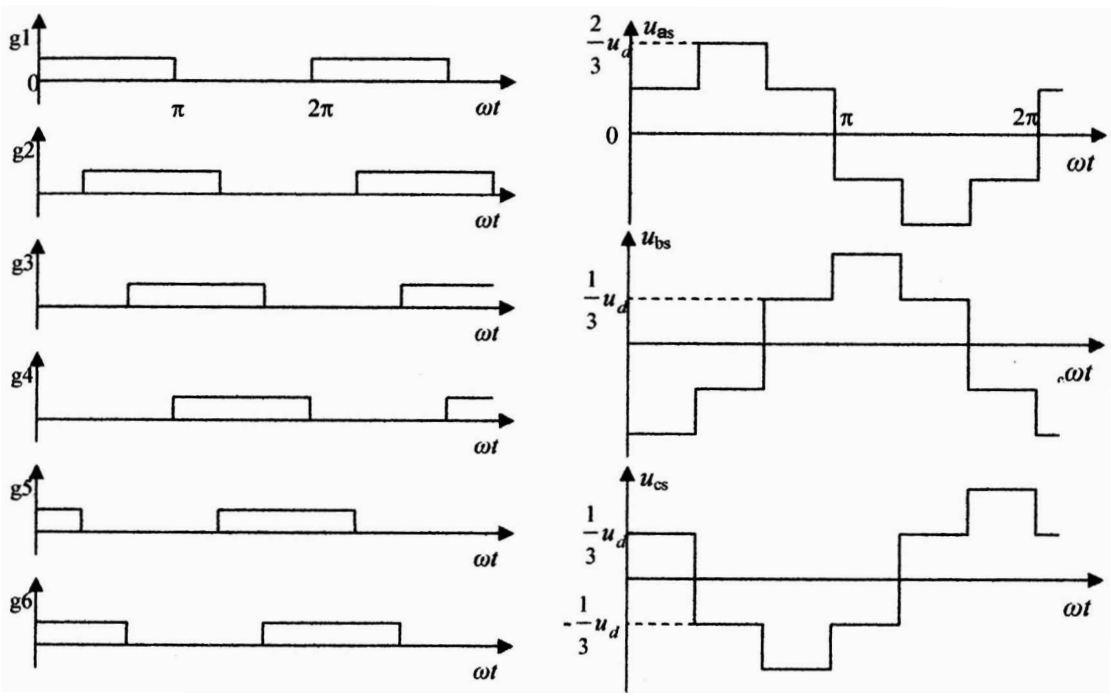

(a) Gating signals (b) Line-to-line voltage waveforms

Figure 2.6: Six-step inverter with 180° conduction angle [1, 5, 7]

2.3.2 Six-step inverter with 120° conduction angle

In this type of control, each thyristor conducts for 120°. Only two thyristors remain on at any instant of time. The sequence of switching is in the order of 6-1, 1-2, 2-3, 3-4, 4-5, 5-6 and back to 6-1 as shown in Figure 2.7(a). This results in the voltage waveforms in Figure 2.7(b).

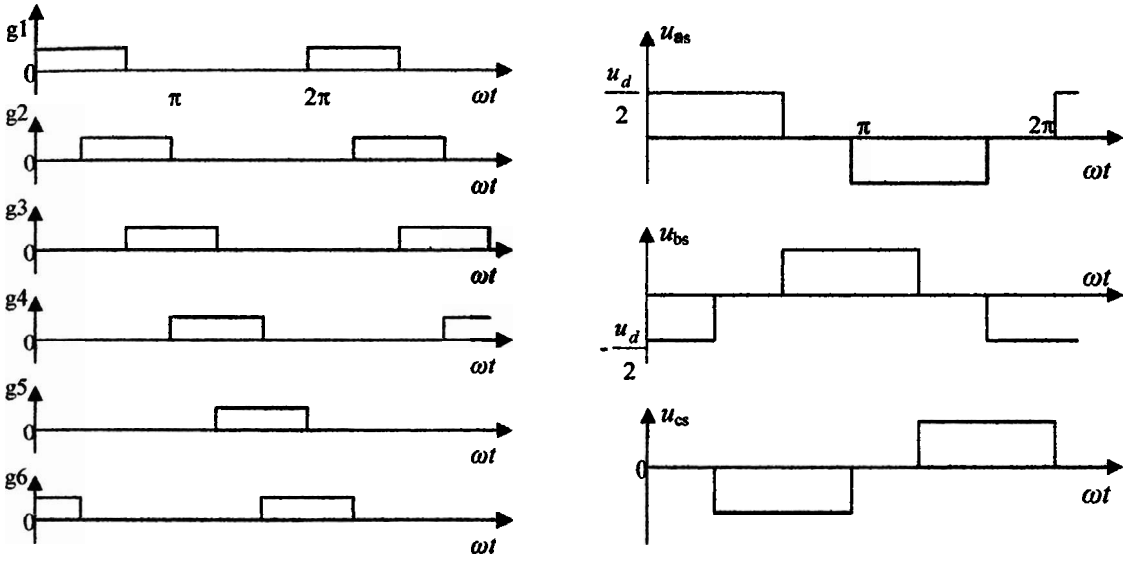

(a) Gating signals (b) Line-to-line voltage waveforms

Figure 2.7: Six-step inverter for 120° conduction angle [5]

2.3.3 PWM inverter

The three-phase bridge inverter circuit for PWM waveform generation is identical to the six-step inverter but the switching sequence is more complex. Voltage control is achieved by modulating the output voltage waveform within the inverter. A wide variety of three-phase PWM techniques has been devised but only sinusoidal PWM is applicable from the simulator.